Nano-ice on Boron Nitride Nanomesh: Accessing Proton Disorder

Haifeng Ma,[a] Thomas Brugger,[a] Simon Berner,[a] Yun Ding,[b] Marcella Iannuzzi,[b] Jürg Hutter,[b] Jürg Osterwalder,[a] and Thomas Greber*[a]

Water was investigated on a h-BN/Rh(111) nanomesh template using variable temperature scanning tunneling microscopy (STM) and density functional theory (DFT) calculations. Below 52 K, two distinct phases self-assemble within the 3.2 nm unit cell of the nanomesh that consists of "holes" and "wires". In the 2 nm holes, an ordered phase of nano-ice crystals with about 40 molecules is found. The ice crystals arrange in a bilayer honeycomb lattice, where hydrogen atoms of the lower layer point to the substrate. The phase on the 1 nm wires is a low density gas phase. Tunneling barrier height dI/dz spectroscopy measurements reveal the dipoles of individual molecules in the nano-ice clusters and access proton disorder.

1. Introduction

Water on surfaces is a long-standing topic of basic science of paramount importance for technological applications.[1,2] The relatively strong hydrogen bonds and dipole moments of water molecules also impose ordering at surfaces, though here too, the protons do not necessarily order into a perfect crystal. This proton disorder is for example, substantial for the understanding of nucleation and growth of ice clusters. For the atomistic understanding of nucleation and growth of water clusters on surfaces, significant progress came from scanning tunneling microscopy experiments at low temperatures.[3,4]

Herein nano-ice clusters are investigated and it is demonstrated that the use of a suitable template, the boron nitride nanomesh, allows self-assembly of ice clusters containing about 40 water molecules. Direct insight in the arrangement of the individual protons in the nano-ice clusters is obtained from the measurement of the local tunneling barriers.

The template, h-BN/Rh(111) nanomesh,[5] is a superstructure based on 12×12 Rh unit cells on top of which 13×13 BN unit cells coincide.[6,7] It is a corrugated single layer of sp²-hybridized hexagonal boron nitride with a super-lattice constant of 3.2 nm. If the nitrogen atom sits close to an on-top position of a substrate Rh atom, h-BN is tightly bound and forms "holes" or "pores" with a diameter of about 2 nm. The loosely bound regions form a connected network and are called "wires". This peculiar morphology implies a functionality which can be used for trapping single molecules.[7] The trapping mechanism was found to be related to the presence of large lateral electric fields in the surface, where the rims of the holes act like dipole rings that lower the electrostatic potential in the holes.[8] Also, it was shown that the h-BN nanomesh is very robust and survives transport in air,[9] immersion into liquids,[7] and even cyclic voltammograms.[10] The impedance analysis in the electrochemical setup suggested that the h-BN nanomesh imposes ordering within the Helmholtz layer of the electrolyte.[10] The lack of a microscopic understanding led us to do experiments where the adsorption of water should be studied with atomic resolution. It turns out that the hydrogen bonds between the water molecules dominate above the bonds to the dipole rings. However, the rims of the holes confine the ice clusters and prevent them from further growth. The wires act like a feeding/draining network that connects the ice clusters and the structure is a nanolaboratory in which many ice clusters may be studied in parallel.

2. Results and Discussion

Figure 1 compares the h-BN/Rh(111) nanomesh with and without adsorbed water. The images with atomic resolution show that water forms a two-phase system, where the two phases coexist in the supercell with 3.2 nm lattice constant. Figure 1a is a large-scale STM current image of the nanostructure (42×42 nm²) across several terraces of the Rh(111) substrate, obtained after dosing about 2 L water on the surface at 52 K. All holes are filled with ice clusters and no ordered water structures appear on the wires. This indicates that in the holes the interaction between water and the surface is strong enough to stabilize molecules. Compared to the empty mesh (Figure 1b), where the holes and the wires are visible as two structural elements of the nanomesh, the holes are filled with small lobes and streaks appear along the scan direction after dosing 1 L of water (Figure 1c). The topographic cross sections across a hole in Figure 1d show water molecules as protrusions with a

[a] Dr. H. Ma, T. Brugger, Dr. S. Berner, Prof. Dr. J. Osterwalder,
Prof. Dr. T. Greber
Institute of Physics
University of Zurich
Winterthurerstrasse 190, 8057 Zurich (Switzerland)
Fax: (+41) 44 635 5704
E-mail: greber@physik.uzh.ch

[b] Y. Ding, Dr. M. Iannuzzi, Prof. Dr. J. Hutter
Institute of Physical Chemistry
University of Zurich
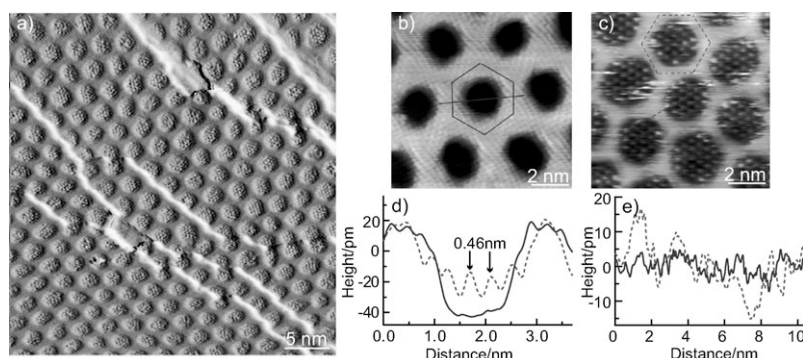Winterthurerstrasse 190, 8057 Zurich (Switzerland)

Figure 1. Nano-ice on the *h*-BN/Rh(111) surface. a) Large-scale STM current image of water molecules adsorbed on the surface at $T = 52$ K. All holes are occupied by distinct ice clusters (42×42 nm^2; $V_s = -0.4$ V; $I_t = 400$ pA). b), c) Atomically-resolved STM topography images of the bare surface and after dosing water (both areas are 9×9 nm^2; and scanning parameters are $V_s = -0.05$ V; $I_t = 100$ pA). d), e) Height profiles across and around the holes in (b) and (c) [——— and •••••, respectively]. The height level 0 in (d) corresponds to the average of (c) and that in (e) to its average.

height of about 15 pm, which is in agreement with the known mapping properties of water on surfaces.[16] The lateral distance between the protrusions is about 0.46 nm in the holes. As we show in the following, it is the signature of a bilayer of water—a lateral honeycomb structure with two sublattices A and B, where molecules in sublattice A form the contrast in the image. Figure 1e shows that the height of the cuts around the wires is irregular, where the height variations are, compared to the empty nanomesh, larger for the water-covered case. We propose that water molecules are moving fast along wires to form a low-density gas phase. These results indicate that the water self-assembly process in the boron nitride nanomesh, separates water into two distinct phases, one on the wires as fuzzy protrusions and one in the holes as ordered nano-ice crystals. Herein, we focus on the structure of the ordered ice clusters.

The lattice constants and the azimuthal orientation can be seen in Figure 2. In Figures 2a,c, STM pictures of two different preparations are shown. The Fourier transforms (Figures 2b,d) reveal the two characteristic lattice constants of the nanomesh (3.2 nm) and the ice clusters (~ 0.46 nm). The lattice constant of ice is 7.0 ± 0.2 times smaller than that of the nanomesh and corresponds within the error bar to that of the basal plane of hexagonal ice (0.45 nm).

For the two shown preparations we find different ice-cluster orientations rotated by $11 \pm 3°$ and $-24 \pm 3°$ with respect to the direction given by two neighboring holes (Figures 2b,d). The observation of rigid ice clusters that are not oriented the same way with respect to the substrate indicate that the lock-in energy of the nano-ice clusters is not as large as the bonding within the ice layer. The histogram in Figure 2e lists the number of molecular protrusions in the 32 holes of Figure 2a where 20 ± 5 protrusions per hole were found. This confirms that water in sublattice A forms the contrast, since a hole with 2.2 nm diameter is expected to host twice as many, that is, about 40 water molecules per bilayer.

Figure 3 substantiates the two sublattice (bilayer) picture with a high-resolution zoom into an ice cluster. The two sub-

lattices A and B were resolved. We assign the highest protrusions A to positions of the topmost oxygen atoms, while the protrusions with intermediate height indicate oxygen atoms of sublattice B. From the cross section in Figure 3b it can be seen that at the given tunneling conditions sublattice B appears about 15 pm below sublattice A. This means that at 34 K ice crystallizes in a bilayer structure, which is also observed for water on Cu(111) after annealing.[17] While it is intuitive to assign the two sublattices to two differently bound water molecules, the topographic images make no direct statement on the positions of the hydrogen atoms, nor the orientation of the lone pairs on the oxygen atoms. In the following we show that the water dipoles and thus the positions of the hydrogen atoms affect the
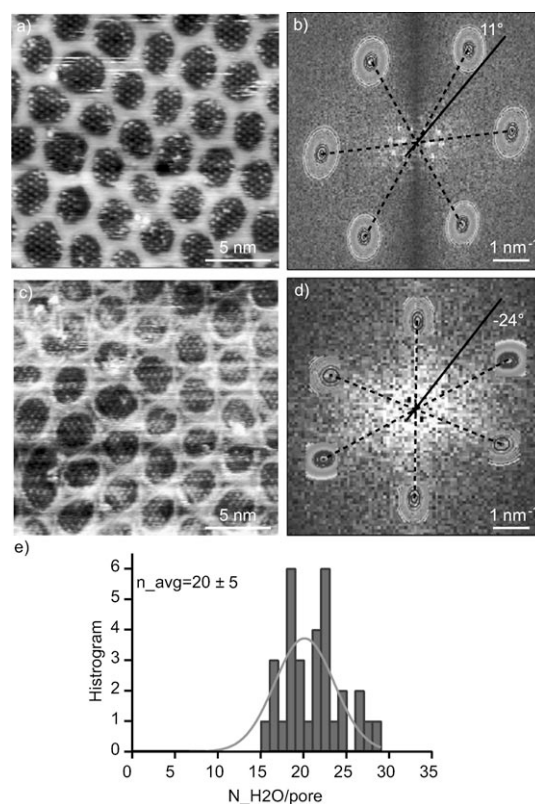

Figure 2. Two different preparations of nano-ice clusters on the surface. a), c) STM topography images of nano-ice on *h*-BN/Rh(111) nanomesh (18×18 nm^2). b), d) The corresponding Fourier transforms of (a) and (c), respectively. The contours of a Gaussian anchor the exact position for the periodicity of water molecules in reciprocal space. The inset angles are corresponding to the orientations between the direction of nano-ice and its neighboring holes. e) The histogram of the numbers of top layer H$_2$O molecules per hole for the area in (a).
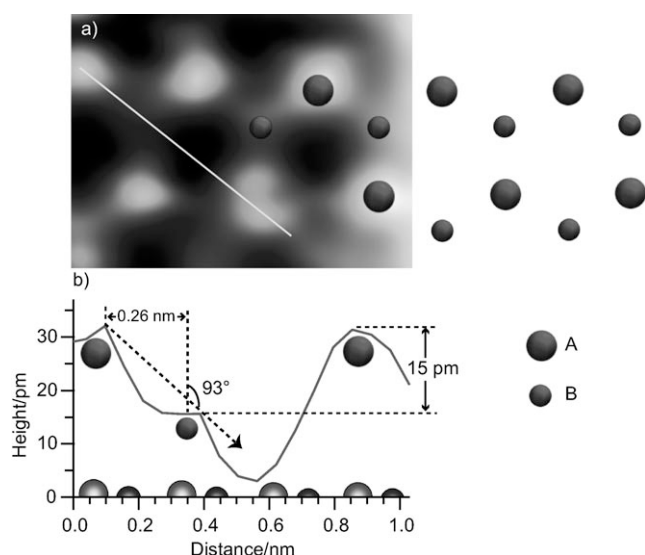
Figure 3. Atomic-scale structure of the nano-ice cluster revealing the honeycomb bilayer with two sublattices A and B. a) High-resolution STM image with the positions of the oxygen atoms (gray balls A and B) are embedded (0.8×1.2 nm²; $V_s = +0.3$ V; $I_t = 100$ pA). b) Height profile across the water molecules in (a) as indicated by the light gray line. The two different water molecules are schematically indicated. The angle between $\overline{AB}$ and the surface normal is 93°.

tunneling barrier. For this purpose, models for the bilayer that obey the ice rules are considered. Essentially the ice rules say that every hydrogen atom forms a hydrogen bond with a neighboring oxygen atom. Every water molecule is modeled by a tetrahedron, with an oxygen atom in the center, two hydrogen atoms or protons in two of its vertices, and two oxygen lone pairs in the two remaining vertices of the tetrahedron.[1] For such an unrelaxed hexagonal bilayer the angle between nearest-neighbor oxygen molecules $\overline{AB}$ and the surface normal is expected to be the tetrahedron angle of 109°.[18] The flattening to the observed 93° may be influenced by local density-of-states effects, the tunneling barrier and the bonding to the substrate.[19] However, the tetrahedron model and the ice rules limit the possible proton arrangements. For a basal hexagram plane that is fully hydrogen bonded, half of the vertices are occupied by hydrogen atoms, and their nearest-neighbor vertices are empty.

The ice rules permit many different arrangements of the protons, that is, allow for a certain proton disorder. In hexagonal bulk ice (I_h) the up and down vertices in the two sublattices host equal numbers of protons and lone pairs. At a surface this is not necessarily the case and it is expected that the up (down) vertices either host a hydrogen atom (lone pair) or vice versa. Here the issue on whether hydrogen atoms in sublattice B point to the substrates or not is addressed by barrier height dI/dz microscopy/spectroscopy,[20,21] since the positions of the ions leave fingerprints in the electrostatic landscape, as it was, for example, shown with image potential state and dI/dV spectroscopy for NaCl layers.[22,23] Electrostatic potential variations locally affect the tunneling barrier height, which is determined in measuring the z-dependence of the tunneling current I that decreases exponentially with the distance z between the tip

and the sample: $I \propto \exp(-z/z_o)$. The decay length z_o depends on the tunneling barrier. For small voltages z_o is roughly proportional to $1/\sqrt{\Phi_l}$, where $\sqrt{\Phi_l}$ is the local work function in the tunneling junction. In the barrier-height microscopy mode the z-position of the tip is oscillated with a given frequency and amplitude, while the tunneling current variations at this frequency are read out, and related via $(d\ln I/dz)^2 \propto \Phi_l$ to the local work function.[20]

Figure 4a shows a corresponding dI/dz map of nano-ice/ h-BN/Rh(111). Clearly, at the positions of the oxygen atoms of sublattice A and on the wires, a larger tunneling barrier is
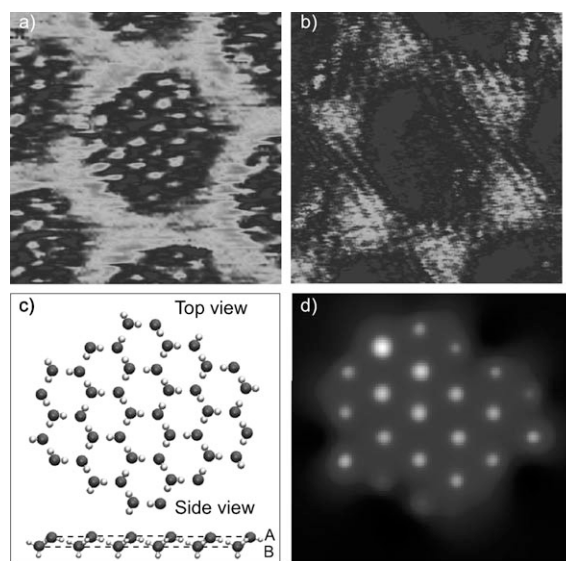

Figure 4. a) The dI/dz map of nano-ice cluster in the hole after dosing 1 L H₂O molecules on the surface. By measuring the response of the tunneling current to the variation of the tunneling gap distance, dI/dz image can be obtained simultaneously with a topographic STM image. For the dI/dz map, the bright colors correspond to large local tunneling barriers (see color bar). b) The dI/dz map was measured on the bare surface (Both images are 6×6 nm²; scanning parameters are $V_s = -0.05$ V; $I_t = 100$ pA). c) Side and top views of the structure model for nano-ice cluster in a single hole. d) The corresponding surface electrostatic potential 0.2 nm above the plane between sublattice A and B in (c) [3×3 nm²].

found, where there is some scatter in the barrier height above the individual oxygen A sites (up vertices). This is consistent with the assignment that the up vertices of sublattice A host oxygen lone pairs and correspondingly that the out-of-plane hydrogen atoms sit on the water molecules of sublattice B and point to the h-BN substrate. Density functional theory calculations of a water molecule on a single sheet of h-BN confirm this picture. They favor single water molecules to bind with the hydrogen to the negatively charged nitrogen atoms.

For comparison we also show the dI/dz map of the bare nanomesh (Figure 4b). This result with atomic resolution on the h-BN is in agreement with the known electrostatic potential energy landscape.[8] Both pictures in Figures 4a,b are recorded with the same tunneling parameters. The magnitude of the lateral local work function variations may be estimated from the measured potential energy difference 0.38 nm above

the *h*-BN of 310 meV between holes and wires in the empty nanomesh.[8]

In order to substantiate the *dI/dz* maps we built bilayer models of ice clusters obeying the above mentioned ice rules together with hydrogen atoms of the lower layer pointing to the substrate. The height difference between the sublattices of 88 pm is taken from DFT calculations of the $(H_2O)_{42}$ cluster on a single layer of *h*-BN. A model of such an ice cluster is shown in Figure 4c. It shows 42 water molecules arranged in a honey-comb fashion, where in sublattice B the hydrogen atoms point to the substrate. Still, there are several possibilities to arrange the hydrogen atoms. Here they are arranged in such a way that the cluster has no lateral dipole moment. From density functional theory we take the Mulliken charges on the oxygen atoms of 0.4 electrons and −0.2 electrons on the hydrogen atoms (protons). With this we calculate the electrostatic potential above the cluster in Figure 4c. Figure 4d shows this potential 0.2 nm above the plane between sublattices A and B. Clearly, the potential that is reminiscent to a local work function is largest on top of the oxygen atoms in sublattice A, that is, on top of the lone pairs that are not saturated with hydrogen atoms. For the chosen parameters we find a corrugation of the electrostatic potential energy landscape of up to 0.8 eV within the cluster. It has to be noted that this energy corrugation is distance-dependent, though 0.8 eV is the order of magnitude of the effect. Calculations of the tunneling barrier at various heights indicate that the *dI/dz* measurements feature the electrostatic potential closer to the surface than adsorbed Xe (0.38 nm), since at a distance of 0.38 nm the molecular resolution is lost.[8] All other proton positions that we modeled, such as a structure with hydrogen atoms pointing to the vacuum, do not produce this kind of agreement. It is interesting to point out that the variations of the tunneling barrier heights on the different water molecules in sublattice A indicate that the method is sensitive to the local arrangement of the dipoles of the water molecules and that this gives access to the direct observation of proton disorder in two dimensional ice clusters. Also, the findings indicate that different proton configurations near the edge of the nano-ice clusters cause electric fields that are important for the understanding of the growth limitation of the clusters and their reaction against other host molecules.

3. Conclusions

We report on the self-assembly of nano-ice clusters with about 40 molecules and a dilute "gas phase" on the *h*-BN/Rh(111) nanomesh template. The nanomesh holes host the clusters and limit their size. With help of DFT and barrier height *dI/dz* spectroscopy the structure of the nano-ice could be refined to that of a hydrogen-bonded honeycomb, where the out-of-plane hydrogen atoms point toward the surface. The positions of the protons in the ice clusters may be inferred from the orientations of the water dipole fields. Nano-ice gives unprecedented insight into the self-assembly of water and indicates it to be a good candidate to study proton disorder in two dimensional ice.

Experimental Section

The experiments were performed in an ultrahigh-vacuum (UHV) chamber with a background pressure below 4×10^{-10} Torr using variable-temperature scanning tunneling microscopy (Omicron VT-STM). The sample preparation included several cycles of Ar⁺-bombardment, subsequent exposure to a few L (1 Langmuir = 10^{-6} Torr s) of O_2 and annealing of the Rh(111) sample. Then it was exposed to 40 L of borazine (HBNH)$_3$ gas, while keeping the surface at 1070 K. This procedure yields a well-ordered large-scale single layer of hexagonal boron nitride on the Rh(111) surface. Milli-Q water was used and purified by several freeze-and-pump cycles. Water was introduced into the UHV chamber via a leak valve in the pressure range of 10^{-10}–10^{-8} Torr through a nozzle pointing towards the sample. All pressures correspond to the uncorrected reading of the ion gauge of the UHV chamber. In order to minimize tip induced H_2O motion on the surface, scanning parameters were set to the order of 50 pA to 400 pA for tunneling currents and −50 mV to −400 mV for tunneling voltages. Tunneling barrier spectroscopy was performed with lock-in technique by superimposing a modulation voltage of 8 mV at 2.0 kHz to the z-piezo. This modulates the tip–sample distance with amplitude of ~0.07 nm. Except for those mentioned explicitly, STM images shown in this paper are obtained at low temperature 34 K.

All the calculations reported here were performed in CP2K[11] with the hybrid Gaussian and plane waves (GPW)[12] method. The revised PBE functional[13] and the Goedecker–Teter–Hutter (GTH)[14] pseudo-potentials for all the DFT calculations were carried out concomitantly, and an additional Grimme[15] potential was added for the dispersion correction.

[1] M. A. Henderson, *Surf. Sci. Rep.* **2002**, *46*, 1–308.
[2] P. A. Thiel, T. E. Madey, *Surf. Sci. Rep.* **1987**, *7*, 211–385.
[3] T. Mitsui, M. K. Rose, E. Fomin, D. F. Ogletree, M. Salmeron, *Science* **2002**, *297*, 1850.
[4] A. Michaelides, K. Morgenstern, *Nat. Mater.* **2007**, *6*, 597–601.
[5] M. Corso, W. Auwärter, M. Muntwiler, A. Tamai, T. Greber, J. Osterwalder, *Science* **2004**, *303*, 217–220.
[6] R. Laskowski, P. Blaha, T. Gallauner, K. Schwarz, *Phys. Rev. Lett.* **2007**, *98*, 106802.
[7] S. Berner, M. Corso, R. Widmer, O. Groening, R. Laskowski, P. Blaha, K. Schwarz, A. Goriachko, H. Over, S. Gsell, M. Schreck, H. Sachdev, T. Greber, J. Osterwalder, *Angew. Chem.* **2007**, *119*, 5207–5211; *Angew. Chem. Int. Ed.* **2007**, *46*, 5115–5119.
[8] H. Dil, J. Lobo-Checa, R. Laskowski, P. Blaha, S. Berner, J. Osterwalder, T. Greber, *Science* **2008**, *319*, 1824–1826.
[9] O. Bunk, M. Corso, D. Martoccia, R. Herger, P. R. Willmott, B. D. Patterson, J. Osterwalder, I. van der Veen, T. Greber, *Surf. Sci.* **2007**, *601*, L7–L10.
[10] R. Widmer, S. Berner, O. Groning, T. Brugger, J. Osterwalder, T. Greber, *Electrochem. Commun.* **2007**, *9*, 2484–2488.
[11] CP2K version 2.0.1 (Development Version), the CP2K developers group (**2009**). CP2K is freely available from http://cp2k.berlios.de/.
[12] G. Lippert, J. Hutter, M. Parrinello, *Mol. Phys.* **1997**, *92*, 477–487.

[13] J. Perdew, K. Burke, M. Ernzerhof, *Phys. Rev. Lett.* **1996**, *77*, 3865–3868.

[14] S. Goedecker, M. Teter, J. Hutter, *Phys. Rev. B* **1996**, *54*, 1703–1710.

[15] S. Grimme, *J. Comput. Chem.* **2006**, *27*, 1787–1799.

[16] T. K. Shimizu, A. Mugarza, J. I. Cerda, M. Heyde, Y. Qi, U. D. Schwarz, D. F. Ogletree, M. Salmeron, *J. Phys. Chem. C* **2008**, *112*, 7445–7454.

[17] M. Mehlhorn, K. Morgenstern, *Phys. Rev. Lett.* **2007**, *99*, 246101.

[18] D. Doering, T. Madey, *Surf. Sci.* **1982**, *123*, 305–337.

[19] H. Ogasawara, B. Brena, D. Nordlund, M. Nyberg, A. Pelmenschikov, L. G. M. Pettersson, A. Nilsson, *Phys. Rev. Lett.* **2002**, *89*, 276102.

[20] R. J. de Vries, A. Saedi, D. Kockmann, A. van Houselt, B. Poelsema, H. J. W. Zandvliet, *Appl. Phys. Lett.* **2008**, *92*, 174101.

[21] Y. Qi, X. Ma, P. Jiang, S. Ji, Y. Fu, J. F. Jia, Q. K. Xue, S. B. Zhang, *Appl. Phys. Lett.* **2007**, *90*, 013109.

[22] M. Pivetta, F. M. C. Patthey, M. Stengel, A. Baldereschi, W. D. Schneider, *Phys. Rev. B* **2005**, *72*, 115404.

[23] F. E. Olsson, M. Persson, J. Repp, G. Meyer, *Phys. Rev. B* **2005**, *71*, 075419.